

Angular distribution of satellite galaxies from the Sloan Digital Sky Survey Data Release 4

Marco Azzaro¹, Santiago G. Patiri², Francisco Prada³, & Andrew R. Zentner⁴

¹ *Universidad de Granada, Av. Fuentenueva s/n, E-18071 Granada, Spain (azzaro@ugr.es)*

² *Instituto de Astrofísica de Canarias, C/Vía Láctea s/n, E-38200, La Laguna, Tenerife, Spain*

³ *Instituto de Astrofísica de Andalucía (CSIC), Apartado Correos 3005, E-18080 Granada, Spain*

⁴ *Kavli Institute for Cosmological Physics & Department of Astronomy and Astrophysics, The University of Chicago, 933 E. 56 St., Chicago, IL 60637, USA*

24 March 2021

ABSTRACT

We explore the angular distribution of two samples of satellite galaxies orbiting isolated hosts extracted from the Sloan Digital Sky Survey Data Release 4. We find a clear alignment of the satellites along the major axis of their hosts when restricting the analysis to red hosts. The anisotropy is most pronounced for red satellites of red hosts. We find that the distribution of the satellites about blue, isolated hosts is consistent with isotropy. We show that under the *assumption* that the true, underlying distribution of satellites of blue hosts exhibits the same anisotropy as the satellites of red hosts, the sample of blue hosts is too small to measure this anisotropy at a statistically-significant level. The anisotropy that we detect for satellites about red primaries is independent of the projected radius. In particular, it is evident at large projected distances from primaries ($300 < r_p < 500$ kpc).

Key words: galaxies: general – galaxies: formation – galaxies: evolution – galaxies: interactions – galaxies: kinematics and dynamics

1 INTRODUCTION

In the standard hierarchical cold dark matter (CDM) model of cosmological structure and galaxy formation (e.g., White & Rees, 1978, Blumenthal et al. 1984), the halos of large galaxies form by the accretion of smaller halos. During this process, some accreted halos may orbit several times within the *host* potential before being incorporated into the central galaxy or severely disturbed by tides (Taffoni et al. 2003, Hayashi et al. 2003, Zentner and Bullock 2003, Kravtsov et al. 2004, Kazantzidis et al. 2004, Taylor Babul 2004, Zentner et al. 2005). The angular distribution of satellites around central hosts carries the imprint of both anisotropic infall (Knebe et al. 2004; Zentner et al. 2005b) during halo formation and the shape of the gravitational potential on the scale of central halos (e.g., Zentner et al. 2005b).

The angular distribution of satellite galaxies has received much recent attention. The topic was first addressed by Holmberg (1969), who found that satellites of spiral galaxies with projected separations $r_p \leq 50$ kpc are preferentially located near the short axes of their host galaxies. Zaritsky et al. (1997) found a statistically-significant anisotropy in the same sense as that of Holmberg (1969), but at larger projected separations ($200 \text{ kpc} \leq r_p \leq 500 \text{ kpc}$). The satellite galaxies of the Local Group exhibit a similar anisotropy

(e.g., Lynden-Bell 1982; Majewski 1994; Hartwick 1996), and this may have important consequences for galaxy formation theory (e.g., Kang et al. 2005; Zentner et al. 2005b; Libeskind et al. 2005).

Sales & Lambas (2004) studied the alignment of satellites with respect to the principal axes of the light distributions of their host galaxies in the Two Degree Field Galaxy Redshift Survey (2dFGRS, Colless et al. 2001). Sales & Lambas (2004) reported a statistically-significant alignment along the minor axes of host galaxies; however, Yang et al. (2006) have since shown that this result was due to a misinterpretation of the Position Angle definition in the 2dFGRS database and that the alignment is actually along host *major* axes. Moreover, the Sales & Lambas (2004) alignment was only in a subsample of hosts with little active star formation and satellites with small velocities relative to their hosts, $\Delta V < 160 \text{ km s}^{-1}$. For a subsample with larger relative velocities ($\Delta V > 160 \text{ km s}^{-1}$), the results of Sales & Lambas (2004) are consistent with isotropy.

Brainerd (2005) studied satellites in the Sloan Digital Sky Survey Data Release 3 (SDSS DR3, e.g. York et al. 2000; Strauss et al. 2002) and also found a preferential alignment of satellites with the major axes of the light distributions of their hosts for $r_p < 100$ kpc. Brainerd (2005) found their

signal to decrease with r_p , reporting a distribution consistent with isotropy for $r_p > 250$ kpc. Brainerd (2005) did not study any dependence upon the spectral or morphological types of the host galaxies. Yang et al. (2006), using groups of galaxies from the SDSS DR2 identified via a halo-based group finder from which halo properties for groups are inferred (Weinmann et al. 2005; Yang et al. 2005), found an alignment of satellites with host major axes, becoming more pronounced at small separations. The strongest alignment was exhibited by red satellites of red hosts and by satellites in massive halos. Azzaro et al. (2005) studied the distribution of satellites in a small subsample of the SDSS sample of Prada et al. (2003) limited to hosts that were morphologically identified as disk galaxies and found no evidence for anisotropy, though the requirement of a morphologically-identified disk primary drove their sample size to be significantly smaller than those of Sales & Lambas (2004), Brainerd (2005), and Yang et al. (2006).

Our aim is to study the angular distribution of satellites about isolated host galaxies with the increased statistics afforded by the SDSS fourth data release (DR4). Our study complements that of Yang et al. (2006), in the sense that we focus on isolated hosts instead of galaxy groups. We refer to central host galaxies as “primary galaxies” or simply “primaries.” Provided primaries are selected in a consistent and homogeneous way, it is useful to consider all satellites as satellites of a single, fictitious primary in order to overcome the small numbers of satellites about individual primaries.

2 DATA AND SELECTION CRITERIA

The data we use are from the latest SDSS public release, DR4. The SDSS is the largest photometric and spectroscopic survey available. CCD imaging covers five colors and spectroscopic follow-up is performed down to $M_r = 17.77$ (York et al. 2000; Stoughton et al. 2002). The SDSS DR4 contains $\sim 411,000$ galaxy spectra distributed on several strips covering $\sim 4,800$ sq. degrees on the sky. The SDSS spectroscopic sample is magnitude limited, though there is some incompleteness due to missing nearby, bright galaxies ($M_r < 15.5$) because of fibre saturation, missing spectra because of fibre collisions (7%; Blanton et al. 2003a), redshift failures ($< 1\%$), and missing galaxies ($\sim 1\%$) close to bright Galactic stars. These effects may bias results for satellites at projected distances $r_p < 100$ kpc from their hosts. For this reason, we perform our analysis on two subsamples. First, we include all satellites with $r_p > 20$ kpc to maximize the sample size while avoiding HII-region or bulge-structure contamination. We repeat the analysis on a subsample of satellites with $r_p > 100$ kpc, and check for consistency. For the purposes of the present work we select two main samples from DR4 and split these into several subsets as we now specify.

Sample 1 is built using the criteria from the first sample of Brainerd (2005): (1) Hosts are at least 2.5 times (1 mag) brighter than any other galaxy within a projected distance $r_p < 700$ kpc and a line-of-sight velocity difference $|dv| < 1000$ km s $^{-1}$; (2) Satellites are at least 6.25 times (2 mag) fainter than their hosts and are found within $r_p < 500$ kpc, and $|dv| < 500$ km s $^{-1}$.

Sample 2 is constructed using the criteria of Sample 2 from Prada et al. (2003), but with a reduced depth of

30000 km s $^{-1}$: (1) Hosts are at least 2 mags brighter than any other galaxy within $r_p < 714$ kpc and $|dv| < 1000$ km s $^{-1}$; (2) Satellites are at least 2 mags fainter than hosts, are found within $r_p < 500$ kpc, and have $|dv| < 500$ km s $^{-1}$ with respect to their hosts. A summary of the sample selection criteria is given in Table 1.

The objects in each sample are subject to the additional criteria that 1) the ellipticity $e > 0.2$ (to ensure that the position angle is well defined), and 2) the primary absolute magnitude is constrained to a bin which we set by inspecting the distribution of primary r magnitudes. This distribution is consistent with a Gaussian with mean -21.99 and standard deviation 0.85 for Sample 1 and mean -21.83 with standard deviation 0.97 for Sample 2. We set the bin to $-23 < M_r < -21$ for both samples.

SDSS DR4 affords larger samples than previous studies. Sample 1 (prior to magnitude restrictions) contains 4522 satellites around 2703 primaries, roughly 30% more than Sales & Lambas (2004) or Brainerd (2005). However, we apply a magnitude selection that reduces the final size of Sample 1 to 3667 satellites which is only slightly ($\sim 13\%$) larger than the aforementioned studies. Though the magnitude constraint lowers our statistics, by limiting the primary absolute magnitudes we aim to select a small range of primary masses so that the systems are comparable in terms of their typical dynamical states, masses, and formation histories.

We split each primary sample into subsets of Red or Blue satellites about either Red or Blue primaries (summarized in Table 2 and Table 4). The $g-r$ color distributions of the primaries and satellites are shown in Fig. 1 for Sample 1 and in Fig. 2 for Sample 2. The bimodality of the distribution is evident (see Strateva et al. 2001, Baldry et al. 2004), with the red peak dominating both the primary and satellite distributions. The local minima between the peaks of the color distributions occur near $g-r = 0.7$ for the primaries and $g-r = 0.6$ for the satellites, and we use these boundaries to construct Blue and Red subsamples of each population.

We assign each satellite an angular position θ , defined as the angle between the primary major axis and the line joining the centre of the primary and the satellite. Exploiting the assumed symmetry, we reduce the angle θ to the first quadrant so that $0^\circ \leq \theta \leq 90^\circ$. We take the Position Angles of the primaries from the SDSS data as the 25-mag-isophote major axis, and compute θ using this Position Angle and the coordinates of the objects. We explicitly confirmed the position angles and θ values for a number of random images of satellite-primary pairs.

3 RESULTS AND CONCLUSIONS

The angular distributions of satellites in Samples 1 and 2 are shown in Fig. 3 and Fig. 4 respectively. The satellites of red primaries show a preferential alignment with the major axes of the primaries. This result is highly significant. The Kolmogorov-Smirnov (KS) probability of drawing the observed population of satellites about red primaries from an isotropic distribution (our null hypothesis) is $P_{KS} \simeq 10^{-4}$ for Sample 1. The satellites of blue primaries have a distribution that is consistent with isotropy. As a consistency test, we calculated the average of the cosines of θ . If the angles

Table 1. Selection criteria for Sample 1 and Sample 2. Primaries ΔM is the minimum difference in r magnitude with the nearest neighbor, Satellites ΔM is the maximum difference in r magnitude with the host; Primaries $|\Delta r_p|$ is the minimum projected distance between primaries, Satellites $|\Delta r_p|$ is the maximum projected distance from the host; Primaries $|\Delta v|$ is the minimum recession velocity difference between hosts, Satellites $|\Delta v|$ is the maximum velocity difference with the host.

Criteria	Sample 1	Sample 2
Primaries ΔM	1.0	2.0
Primaries $ \Delta r_p $	< 700 kpc	< 714 kpc
Primaries $ \Delta v $	< 1000 km s ⁻¹	< 1000 km s ⁻¹
Satellites ΔM	2.0	2.0
Satellites $ \Delta r_p $	< 500 kpc	< 500 kpc
Satellites $ \Delta v $	< 500 km s ⁻¹	< 500 km s ⁻¹

Table 2. Distribution of the objects in Sample 1 (top) and Sample 2 (bottom).

Color of primaries	N. of primaries	N. of satellites
Blue	523	675
Red	1722	2992
Tot	2245	3667
Blue	312	378
Red	700	985
Tot	1012	1363

were randomly distributed, this average would tend to $2/\pi$. Proximity to this average is then translated into a probability for drawing the sample from an isotropic distribution. A summary of the results of the KS and Cosine tests is shown in Table 3.

The satellites of the blue galaxies are consistent with isotropy in all cases. To determine whether or not the sample size of satellites about blue primaries is large enough

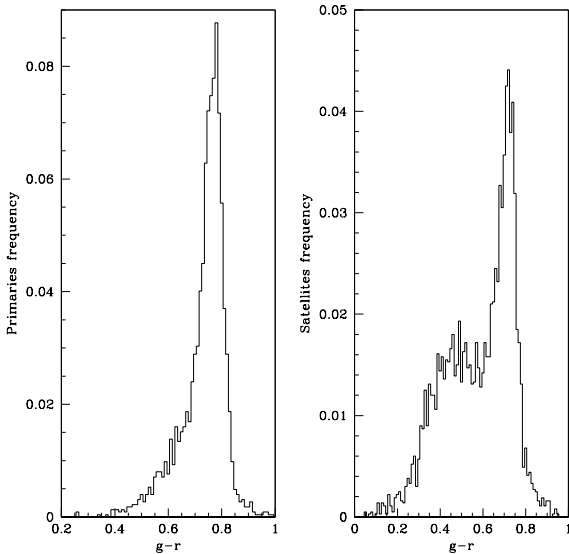


Figure 1. The $g - r$ color distribution of the primaries and the satellites in Sample 1.

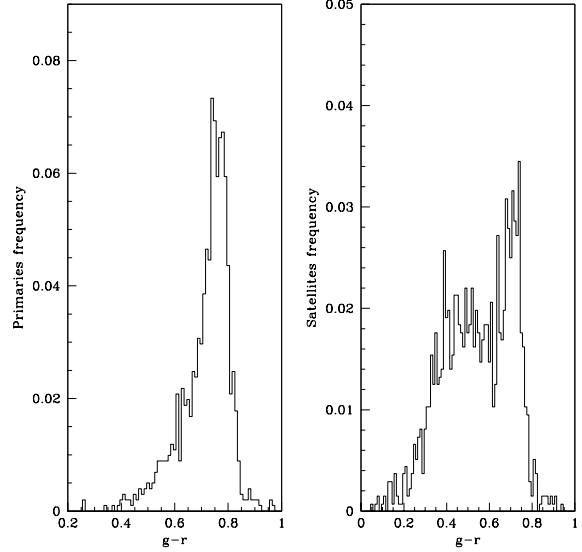


Figure 2. Same as Fig. 1 but for Sample 2

Table 3. Results of the Kolmogorov-Smirnov and Cosine tests. Probabilities (either KS or Cosine) are for the satellites angular distribution to be drawn from an isotropic distribution. The Subsets are indicated with S1 or S2 for Sample 1 or Sample 2, “blue” or “red” refer to the primary color, while “RedBlue” indicates the blue satellites of red primaries, and “RedRed” indicates the red satellites of red primaries. The second column shows the low limit of the projected distance r_p for the Subset.

Subset	r_p min. (kpc)	KS prob.	Cosine prob.
S1blue	20	0.992	0.998
S1blue	100	0.979	0.678
S1blue	300	0.885	0.979
S2blue	20	0.954	0.866
S2blue	100	0.931	0.551
S2blue	300	0.613	0.473
S1red	20	2.3×10^{-4}	2.4×10^{-4}
S1red	100	7.6×10^{-4}	3.9×10^{-4}
S1red	300	4.9×10^{-3}	6.9×10^{-3}
S2red	20	1.0×10^{-2}	5.9×10^{-2}
S2red	100	1.6×10^{-2}	3.3×10^{-2}
S2red	300	0.1	6.1×10^{-2}
S1RedBlue	100	0.302	0.479
S1RedRed	100	1.4×10^{-4}	2.0×10^{-5}

to detect a statistically-significant anisotropy *assuming* the anisotropy to be at the same level as that of the red sample, we drew ten random subsamples of 675 satellites from the 2992 satellites of red primaries in Sample 1. KS tests performed on the random subsamples returned KS probabilities of order tens of percent relative to isotropic. This is indicative that the size of the blue sample is insufficient to detect anisotropy assuming that the underlying distribution exhibits anisotropy at the same level as that of the red primary sample.

The right panels of Fig. 3 and Fig. 4 show the mean angle $\langle \theta \rangle$, as a function of projected distance. These figures indicate that there is no clear dependence of θ on r_p for

Table 4. Satellite numerical distribution in Sample 1 (top) and Sample 2 (bottom).

Prim. color	Satell. color	N. of prim.	N. of satell.
Blue	Blue	426	504
Red	Blue	921	1186
Blue	Red	141	168
Red	Red	1127	1800
Blue	Blue	267	303
Red	Blue	405	478
Blue	Red	65	72
Red	Red	388	504

any subsample. The innermost points at $r_p = 25$ kpc depart from the mean distribution, showing greater anisotropy, but this discrepancy is not statistically significant and may be partially caused by incompleteness in pairs at small separations and it is possible that such systematics may cause the feature found by Brainerd (2005) in the same range of r_p . To mitigate any systematics associated with pairs at small separations, we repeated this analysis with subsamples of satellites with $r_p > 100$ kpc and confirmed the above results.

The alignment of satellites that we report is broadly consistent with that of Brainerd (2005), Yang et al. (2006), and Sales-Lambas (2004, after correction by Yang et al. 2006). Brainerd (2005) gave no indication of a color dependence for this alignment, while Sales & Lambas (2004) mention that satellites of primaries with low star-formation rates exhibit the strongest anisotropy, in qualitative agreement with our alignment for satellites of red primaries. Brainerd (2005) found that anisotropy was more pronounced at $r_p < 100$ kpc and vanished at $r_p > 250$ kpc. We find clear evidence for anisotropy in satellites with $100 < r_p < 300$ kpc and $300 < r_p < 500$ kpc. The satellites of the red primaries of Sample 1 in these ranges yield $P_{KS} \simeq 5 \times 10^{-2}$ and $P_{KS} \simeq 5 \times 10^{-3}$ respectively. Sales & Lambas (2004) report a signal only when restricting to $|\Delta v| < 160$ km s $^{-1}$, whereas we apply no restriction in that sense yet measure significant anisotropy. Lastly, Yang et al. (2006) use a sample of galaxy groups, while we select only isolated systems.

We also studied satellite angular distributions making a rough separation into Blue and Red satellites (subsamples in Table 4). Some of the subsets contain relatively few objects, making robust, statistical comparisons between different populations difficult. Generally, red primaries have more satellites than blue primaries, red primaries have more red satellites than blue satellites, and there are few blue primaries with red satellites, as expected. As an example, the angular distributions of blue and red satellites about red primaries of Sample 1 are shown in Fig. 5. These results extend those of Yang et al. (2006) to include isolated systems. We find the most significant major axis alignment for red satellites of red primaries ($P_{KS} = 1.4 \times 10^{-4}$). We find that the satellites of blue primaries (either red or blue) seem to be consistent with isotropy but note that there are significantly fewer blue primaries.

Concerning the presence of interlopers (galaxies not bound to their assigned primary, but classified as satellites due to projection effects) in our samples, we could be affected by a contamination of the order of 10% (as estimated by Prada et al. 2003). However, interlopers should not be associated with specific primaries in any meaningful way so

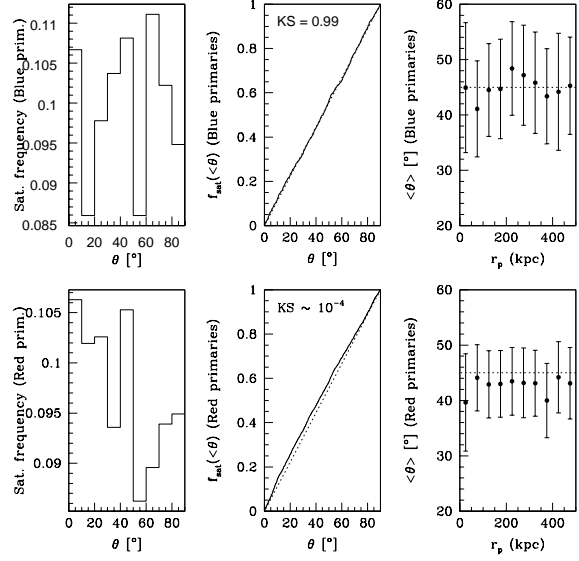


Figure 3. Distribution of the satellites with $r_p > 20$ kpc. The left panels show the probability distribution of angular position for the satellites of Sample 1 that reside around primaries with $-23 < M_r < -21$. Center panels show the cumulative angular distributions and the KS probabilities for drawing the observed distribution from an isotropic distribution (our null hypothesis). Right panels show the mean angular position (θ) as a function of r_p , where the errorbars indicate the error on the mean. The top row of panels shows distributions for satellites about Blue primaries ($g - r < 0.7$) and the bottom row of panels shows satellites around Red primaries ($g - r > 0.7$).

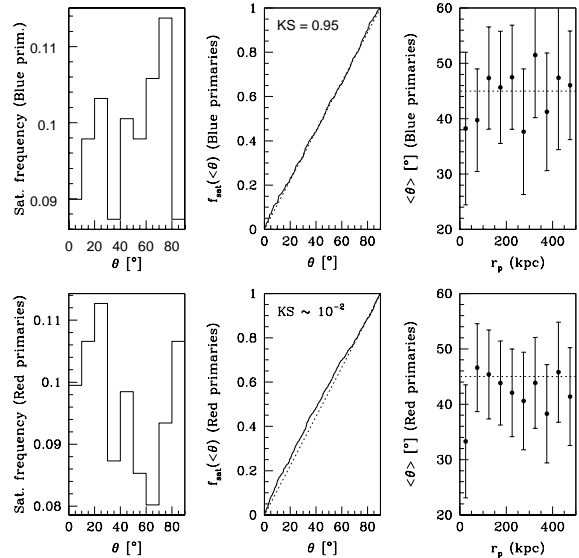


Figure 4. Same as Fig. 3 but for Sample 2.

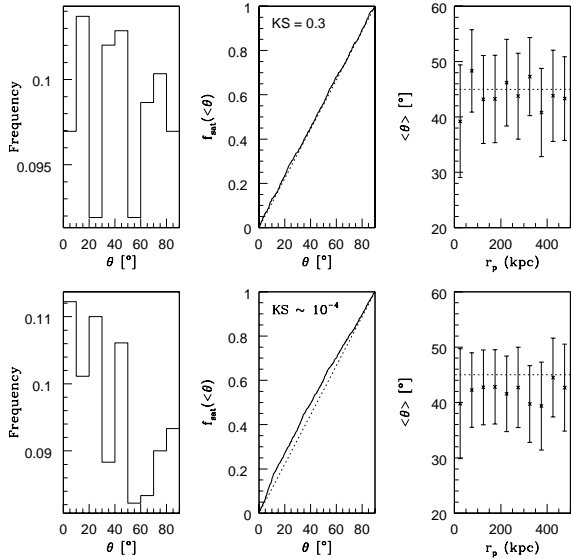


Figure 5. Same as Fig. 3, but for Blue (top row) and Red (bottom row) satellites of only the Red primaries of Sample 1.

that they should only serve to dilute the anisotropy that we measure. In fact, Azzaro et al. (2005) demonstrated this explicitly on mock catalogs constructed from cosmological numerical simulations. Therefore, our findings should only be reinforced upon undertaking some (reliable) method for interloper removal.

Broadly speaking, we confirm the major axis alignment recently found by other authors. In particular, we extend the results of Yang et al. (2006) to isolated systems. We find that angular distributions depend on both primary and satellite color. Red primaries have anisotropic satellite distributions with satellites aligned with the major axes of their hosts and red satellites of red primaries show the strongest such alignment. Blue primaries have distributions consistent with isotropy. However, we have shown that the sample size of blue primaries is insufficient to detect any anisotropy *assuming* an underlying distribution with the same level of anisotropy as the red primary sample. We determine this by constructing random subsamples of the population of satellites about red primaries that had the same size as the sample of satellites about blue primaries and re-analyzing these subsamples as independent samples. Unlike Brainerd (2005) and Sales & Lambas (2004), we find a statistically-significant anisotropy for satellites at both large projected separations $r_p > 300$ kpc and large relative velocities $|\Delta v| > 160$ km/s indicating that this preferential alignment is a rather general feature of satellites about red, or early-type primaries.

ACKNOWLEDGEMENTS

We wish to thank Juan Betancort-Rijo for useful discussions.

SGP & FP are supported by the Spanish MEC under grant PNAYA 2005-07789.

ARZ is supported by the Kavli Institute for Cosmological Physics at The University of Chicago and by the National Science Foundation under grant NSF PHY 0114422.

REFERENCES

- Azzaro M., Zentner A.R., Prada F. & Klypin A.A., 2005, astro-ph/0506547
- Baldry I. K., Glazebrook K., Brinkmann J., Ivezić Ž., Lupton R. H., Nichol R. C. & Szalay A. S. 2004, ApJ, 600, 681-694
- Blumenthal, G. R., Faber, S. M., Primack, J. R., & Rees, M. J. 1984, Nature, 311, 517
- Blanton, M. R., Lin, H., Lupton, R. H., Maley, F. M., Young, N., Zehavi, I., & Loveday, J. 2003a, AJ, 125, 2276
- Brainerd T. G., 2005, ApJ, 628 iss. 2, L101
- Colless, M., Dalton, G., Maddox, S., Sutherland, W., & the 2dF collaboration. 2001, MNRAS, 328, 1039
- Hartwick, F. D. A. 1996, in ASP Conf. Ser. 92, Formation of the Galactic Halo... Inside and Out, 444
- Hayashi, D., Navarro, J. F., Taylor, J. E., Stadel, J., & Quinn, T. 2003, ApJ, 584, 541
- Holmberg E., 1969, Arkiv Astron., 5, 305
- Kang, X., Mao, S., Gao, L., Jing, Y. P. 2005, A&A, 437, 383
- Kazantzidis, S., Mayer, L., Mastroiello, C., Diemand, J., Stadel, J., & Moore, B. 2004, ApJ, 608, 663
- Knebe, A., Gill, S. P. D., Gibson, B. K., Lewis, G. F., Ibata, R. A., and Dopita, M. A. 2004, ApJ, 603, 7
- Kravtsov, A. V., Gnedin, O. Y., & Klypin, A. A. 2004, ApJ, 609, 482
- Libeskind, N. I., Frenk, C. S., Cole, S., Helly, J. C., Jenkins, A., Navarro, J. F., Power, C. 2005, MNRAS, 363, 146
- Lynden-Bell, D. 1982, Obs., 102, 202
- Majewski, S. R. 1994, ApJL, 431, L17
- McKay, T. A., Sheldon, E. S., Johnston, D., Grebel, E. K., Prada, F., Rix, H., Bahcall, N. A., Brinkmann, J., Csabai, I., Fukugita, M., Lamb, D. Q., & York, D. G. 2002, ApJL, 571, L85
- Prada, F., Vitvitska, M., Klypin, A., Holtzman, J. A., Schlegel, D. J., Grebel, E. K., Rix, H.-W., Brinkmann, J., McKay, T. A., & Csabai, I. 2003, ApJ, 598, 260
- Sales L. & Lambas D. G., 2004, MNRAS, 348, 1236
- Stoughton, C. et al. 2002, AJ, 123, 485
- Strateva I. & 28 coauthors, 2001, AJ, 122, 1861-1874
- Strauss, M. A., Weinberg, D. H., Lupton, R. H., & the SDSS collaboration. 2002, AJ, 124, 1810
- Taffoni, G., Mayer, L., Colpi, M., & Governato, F. 2003, MNRAS, 341, 434
- Taylor, J. E. & Babul, A. 2004, MNRAS, 348, 811
- Weinmann, S. M., van den Bosch, F. C., Yang, X., & Mo, H. J. 2005, MNRAS Accepted, astro-ph/0509147
- White, S. D. M. & Rees, M. J. 1978, MNRAS, 183, 341
- Yang, X., Mo, H. J., van den Bosch, F. C., & Jing, Y. P. 2005, MNRAS, 356, 1293
- Yang, X., van den Bosch, F. C., Mo, H.J., Mao, S., Kang, X., Weinmann, S. M., Guo, Y. & Jing, Y. P., MNRAS, submitted, astro-ph/0601040
- York, D. G., Adelman, J., Anderson, J. E., Anderson, S. F., Annis, J., & the SDSS collaboration. 2000, AJ, 120, 1579
- Zaritsky D., Smith R., Frenk C. S. & White S. D. M., 1993, ApJ, 405, 464-478
- Zaritsky D., Smith R., Frenk C. S. & White S. D. M., 1997, ApJL, 478, L53
- Zentner, A. R., Berlind, A. A., Bullock, J. S., Kravtsov, A. V., & Wechsler, R. H. 2005a, ApJ, 624, 505
- Zentner, A. R. & Bullock, J. S. 2003, ApJ, 598, 49
- Zentner, A. R., Kravtsov, A. V., Gnedin, O. Y., & Klypin, A. A. 2005b, ApJ, 629, 219

